Invited Feature Article

Water Dynamics and Proton Transfer in Nafion Fuel Cell Membranes

David E. Moilanen, D. B. Spry, and M. D. Fayer*

Department of Chemistry, Stanford University, Stanford, California 94305

Received October 27, 2007. In Final Form: December 9, 2007

The dynamics of water and its effect on proton transport kinetics in Nafion membranes are compared at several hydration levels. Nafion is the most widely used polyelectrolyte membrane in fuel cells. Ultrafast infrared spectroscopy of the O−D stretch of dilute HOD in H_2O provides a probe of the local environment and hydrogen bond network dynamics of water confined in the hydrophilic regions of Nafion. The kinetics of proton transfer in Nafion are tracked by following the excited-state proton transfer and recombination kinetics of a molecular probe, pyranine (HPTS). The hydrophilic domains of Nafion grow with increased hydration, and the interfacial regions reorganize, leading to a changing local environment for water near the interface. Swelling is not uniform throughout the membrane, and heterogeneity is observed in the fluorescence anisotropy decays of the methoxy derivative of pyranine. Measurements of the time-dependent anisotropy of water in Nafion provide a direct probe of the hydrogen bond network dynamics. These dynamics, as well as the rate of proton transport over nanoscopic distances, are observed to slow significantly as the hydration level of the membrane decreases. The results provide insights into the influence of changes in the dynamics of water on the proton-transfer processes.

I. Introduction

Over the past three decades, a significant amount of effort has been directed toward understanding the structure and proton-transport properties of Nafion, a polyelectrolyte membrane.[1−17] Nafion was originally developed by DuPont for use in chloralkali technologies[18] but has since become the most commonly used membrane separator in polymer electrolyte membrane fuel cells. The reasons for Nafion's success as a fuel cell membrane lie in its robust structure and high proton conductivity, allowing it to function in the harsh conditions required for fuel cell operation without quickly deteriorating. Nafion is a polymer consisting of a fluorocarbon backbone with pendent side chains terminated with sulfonate groups (Figure 1). The extreme difference in the polarity of the fluorocarbon backbone and the sulfonate groups causes the polymer to segregate itself into hydrophilic and hydrophobic domains. The hydrophilic regions are quite hygroscopic and readily absorb water, which hydrates the sulfonate groups. The water contained in Nafion's nanoscopic "channels" is the medium that allows protons to diffuse from the anode to the cathode of a fuel cell.

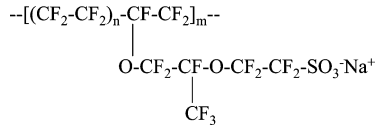

Figure 1. Repeat structure of Nafion. *n* can vary between 5 and 14, but for 1100 EW Nafion, $n = 7$. *m* is typically on the order of 1000.

A significant amount of research effort has been devoted to characterizing the structure of the hydrophilic domains of Nafion. Early models described the structure as reverse micellar-like clusters of sulfonate groups that swelled as water was absorbed into the membrane and eventually allowed proton transfer through small channels connecting the clusters.[2] Later models described the hydrophilic domains as irregular interconnected channels, highlighting the heterogeneity of the polymeric structure.[3,11] Recent scattering experiments have provided a more detailed description of Nafion as consisting of fibrillar aggregates of a fluorocarbon backbone with the hydrophilic sulfonate side chains protruding radially outward.[8,9] These fibrillar structures pack together with the hydrophilic groups of one fiber close to those of its neighbors. Water uptake results in increased space between the fibers leading to irregular channels as proposed in earlier studies.[3,11]

The changing topology of the hydrophilic domains, their size, and the nature of the interfacial region play an important role in mediating the proton transport through the membrane. Proton transport, both by the vehicle mechanism and the Grotthüs mechanism, depends on the nature and dynamics of the hydrogen-bonding network of water.[19] In proton transport by the vehicle mechanism, the proton is carried by a single hydronium ion that

* To whom correspondence should be addressed. E-mail: fayer@stanford.edu.

(1) Yeo, S. C.; Eisenberg, A. *J. Appl. Polym. Sci.* **1977**, *21*, 875−898.
(2) Gierke, T. D.; Munn, G. E.; Wilson, F. C. *J. Polym. Sci.: Polym. Phys. Ed.* **1981**, *19*, 1687−1704.
(3) Falk, M. *Can. J. Chem.* **1980**, *58*, 1495−1501.
(4) Zawodzinski, T. A.; Neeman, M.; Sillerud, L. O.; Gottesfeld, S. *J. Phys. Chem.* **1991**, *95*, 6040−6044.
(5) Kreuer, K.-D.; Dippel, T.; Meyer, W.; Maier, J. *Mater. Res. Soc. Symp. Proc.* **1993**, *293*, 273−282.
(6) Gebel, G. *Polymer* **2000**, *41*, 5829−5838.
(7) Gebel, G.; Lambard, J. *Macromolecules* **1997**, *30*, 7914−7920.
(8) Rubatat, L.; Gebel, G.; Diat, O. *Macromolecules* **2004**, *37*, 7772−7783.
(9) Rubatat, L.; Rollet, A. L.; Gebel, G.; Diat, O. *Macromolecules* **2002**, *35*, 4050−4055.
(10) MacMillan, B.; Sharp, A. R.; Armstrong, R. L. *Polymer* **1999**, *40*, 2471−2480.
(11) Yeager, H. L.; Steck, A. *J. Electrochem. Soc.* **1981**, *128*, 1880−1884.
(12) Paddison, S. J.; Paul, R. *Phys. Chem. Chem. Phys.* **2002**, *4*, 1158−1163.
(13) Pivovar, A. M.; Pivovar, B. S. *J. Phys. Chem. B* **2005**, *109*, 785−793.
(14) Cui, S.; Liu, J.; Selvan, M. E.; Keffer, D. J.; Edwards, B. J.; Steele, W. V. *J. Phys. Chem. B* **2007**, *111*, 2208−2218.
(15) Petersen, M. K.; Voth, G. A. *J. Phys. Chem. B* **2006**, *110*, 18594−18600.
(16) Spry, D. B.; Goun, A.; Glusac, K.; Moilanen, D. E.; Fayer, M. D. *J. Am. Chem. Soc.* **2007**, *129*, 8122−8130.
(17) Devanathan, R.; Venkatnathan, A.; Dupuis, M. *J. Phys. Chem. B* **2007**, *111*, 8069−8079.
(18) Hora, C. J.; Maloney, D. E. *J. Electrochem. Soc.* **1977**, *124*, C319.

10.1021/la703358a CCC: $40.75
Published on Web 01/26/2008

moves with the diffusion constant of water. The Grotthüs mechanism involves proton hopping between adjacent water molecules with proton transfer occurring through the hydrogen-bonding network rather than by the movement of a single hydronium ion. As the size and shape of the hydrophilic domains in Nafion change, the nature of the hydrogen-bonding network changes, and the ability of the water network to transport protons also changes. Neutron scattering[13] and NMR[5] diffusion measurements show that the diffusion of water and protons depends strongly on the level of membrane hydration. At low hydration levels, proton diffusion occurs primarily through the vehicle mechanism because there are not enough water molecules solvating the proton to allow the formation of the extended networks necessary for the Grotthüs mechanism.[5] As the level of hydration increases, proton diffusion also increases but never reaches the value of bulk water because of the geometrical restrictions on the hydrogen-bonding network.[5] Recent MD simulations provide a similar picture of hydronium ions interacting strongly with the sulfonate groups, leading to low rates of proton diffusion at low water content.[12,14,15,17] As the hydration of the membrane increases, more water becomes available to solvate the hydronium ion, allowing an increase in Grotthüs diffusion.

The nature of the aqueous environment may also be investigated with molecular probes or by studying the infrared spectrum of the absorbed water directly. Several groups have utilized a variety of molecular probes to study the hydrophilic domains in Nafion.[20−24] Most of these studies investigated fully hydrated or completely dry Nafion and did not address the question of how the membrane changes with hydration. A major consideration in the use of molecular probes is in determining how they partition between the aqueous environment and the nonpolar environment. Many previous studies used nonpolar or slightly polar probe molecules that may reside in a wide range of locations within Nafion, from the center of the aqueous domains to the interfacial regions.

Infrared spectroscopic studies of water in Nafion can provide information about the environment experienced by the absorbed water molecules but are complicated by the broad, strong absorption from the sulfonic acid groups of protonated Nafion that can overwhelm other signals in all but the thinnest membranes.[25] This complication can be avoided by substituting Na^+ for the protons, which is possible because Nafion can exchange its protons for a variety of other cations. The drawback in this substitution is that the hydrophilic domains are no longer identical to those in working fuel cells that use Nafion in the protonated state. Previous infrared studies of water in Nafion have often utilized pure H_2O, which has a complicated spectrum consisting of many overlapping bands.[25,26] In one of the earliest IR experiments on Nafion, Falk reported spectra of dilute HOD in Nafion greatly simplifying the interpretation of the spectra. However, the results were reported at only two hydration levels.[3] Recently, the first ultrafast infrared pump−probe experiments

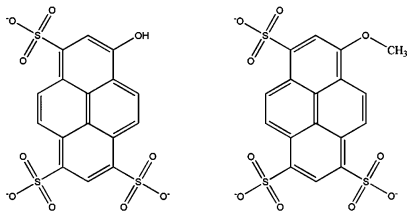

Figure 2. Structures of pyranine (1-hydroxy-3,6,8-pyrenetrisulfonic acid, commonly referred to as HPTS) and MPTS, the methoxy derivative of HPTS.

were conducted on water in Nafion membranes. These experiments provide a direct measurement of the water dynamics.[27,28]

Here we present the results of infrared and fluorescence studies of the properties of water and the kinetics of proton transport in the hydrophilic regions of Nafion at hydration levels ranging from dry to fully hydrated. The infrared experiments probe the O−D stretch of dilute HOD in H_2O, which provides a local observable to monitor changes in the environment experienced by the water as well as a direct probe of the dynamics of the hydrogen-bonding network. Studying dilute HOD simplifies the infrared spectrum by eliminating Fermi resonances and complications arising from the overlapping symmetric and antisymmetric stretching modes of pure H_2O and D_2O. In addition, the study of dilute HOD eliminates vibrational excitation transfer[29] (a major problem in studying pure H_2O or D_2O). In the absence of excitation transfer, polarization-selective pump−probe experiments can be used to directly monitor the orientational motions of the water molecules in nanoscopic environments.[28,30,31]

The fluorescence experiments utilize molecular probes 8-hydroxypyrene-1,3,6-trisulfonate (HPTS) and its methoxy derivative 8-methoxypyrene-1,3,6-trisulfonate (MPTS). The structures are given in Figure 2. HPTS is a photoacid, a molecule that undergoes a large change in pK_a upon electronic excitation. In its ground state, HPTS has a pK_a of 7.7 and is almost fully protonated in neutral water. Upon electronic excitation, the pK_a of HPTS drops by approximately 7 units, and it rapidly transfers its phenolic proton to the surrounding water.[32,33] The ability of the water to solvate the proton and move it away from the excited HPTS molecule depends strongly on the hydrogen bond dynamics, which are closely related to the reorientational dynamics, of water in the vicinity of the photoacid. In addition to its ability to transfer a proton to the surrounding water upon photoexcitation, HPTS has the added advantage that its −3 formal charge partitions it in the center of the aqueous domain, as far from the sulfonate groups at the interface as possible.[34−36] Employing HPTS and MPTS in these experiments eliminates the uncertainty in previous experiments of where the probe molecule resides.

The combination of direct dynamical measurements of water and the use of a photoacid molecular probe in the aqueous domains

(19) Voth, G. A. *Acc. Chem. Res.* **2006**, *39*, 143−150.
(20) Mukherjee, T. K.; Datta, A. *J. Phys. Chem. B* **2005**, *110*, 2611−2617.
(21) Szentirmay, M. N.; Prieto, N. E.; Martin, C. R. *J. Phys. Chem.* **1985**, *89*, 3017−3023.
(22) Lee, H. W. H.; Huston, A. L.; Gehrtz, M.; Moerner, W. E. *Chem. Phys. Lett.* **1985**, *114*, 491.
(23) Kalyanasundaram, K.; Thomas, J. K. *J. Am. Chem. Soc.* **1977**, *99*, 2039−2044.
(24) Kuczynski, J. P.; Milovsavljevic, B. H.; Thomas, J. K. *J. Phys. Chem.* **1984**, *84*, 980−984.
(25) Iwamoto, R.; Oguro, K.; Sato, M.; Iseki, Y. *J. Phys. Chem. B* **2002**, *106*, 6973−6979.
(26) Laporta, M.; Pegoraro, M.; Zanderighi, L. *Phys. Chem. Chem. Phys.* **1999**, *1*, 4619−4628.
(27) Moilanen, D. E.; Piletic, I. R.; Fayer, M. D. *J. Phys. Chem. A* **2006**, *110*, 9084−9088.
(28) Moilanen, D. E.; Piletic, I. R.; Fayer, M. D. *J. Phys. Chem. C* **2007**, *111*, 8884−8891.
(29) Gaffney, K. J.; Piletic, I. R.; Fayer, M. D. *J. Chem. Phys.* **2003**, *118*, 2270−2278.
(30) Piletic, I. R.; Moilanen, D. E.; Spry, D. B.; Levinger, N. E.; Fayer, M. D. *J. Phys. Chem. A* **2006**, *110*, 4985−4999.
(31) Tan, H.-S.; Piletic, I. R.; Fayer, M. D. *J. Chem. Phys.* **2005**, *122*, 174501−174509.
(32) Spry, D. B.; Goun, A.; Fayer, M. D. *J. Chem. Phys.* **2006**, *125*, 144514.
(33) Leiderman, P.; Genosar, L.; Huppert, D. *J. Phys. Chem. A* **2005**, *109*, 5965−5977.
(34) Bardez, E.; Goguillon, B.-T.; Keh, E.; Valeur, B. *J. Phys. Chem.* **1984**, *88*, 1909−1913.
(35) Kondo, H.; Miwa, I.; Sunamoto, J. *J. Phys. Chem.* **1982**, *86*, 4826−4831.
(36) Politi, M. J.; Chaimovich, H. *J. Phys. Chem.* **1986**, *90*, 282−287.

of Nafion provides a powerful approach for characterizing the changing nature of the hydrophilic domains, the dynamics of the hydrogen-bonding network, and the processes affecting nanoscopic proton transfer. It is well known that proton transfer is highly dependent on the orientational motions of water molecules and the dynamics of the hydrogen-bonding network as a whole. A measurement of the time-dependent anisotropy of water provides a direct observation of the hydrogen bond dynamics. These measurements, in conjunction with the use of photoacids to trigger and monitor the kinetics of proton transfer, allow a direct connection to be made between the water dynamics and proton transfer.

II. Experimental Procedures

A. Samples and Time-Independent Spectroscopy. Nafion-117 samples were purchased from Fuelcellstore.com in the acid form. Samples were converted to the sodium form by soaking in a 1 M NaCl solution for 24 h followed by a deionized water rinse and were used without further purification. For the fluorescence experiments, the Nafion samples were boiled for 24 h in an ~0.1 M solution of HPTS or MPTS (Figure 2) to incorporate the molecular probe into the membrane. A homebuilt humidity control system was used to equilibrate the samples under constant relative humidity conditions. First, the membrane is dried by heating in dry air (dew point − 100 °C). Then dry air is bubbled through a water reservoir containing dilute (<5%) HOD in H_2O. The reservoir is maintained at various constant temperatures to produce relative humidities ranging from 0 to 100%. The humidified air purges a Plexiglas box that has a humidity meter to monitor the relative humidity and glove ports for sample manipulation and preparation. The number of water molecules per sulfonate group, λ, was determined by measuring the mass uptake of a Nafion membrane as a function of relative humidity.

After samples reached the proper hydration level, they were sealed in sample cells between 3-mm-thick CaF_2 windows separated by a 200 μm Teflon spacer. A similar procedure was followed for the fluorescence experiments, but the samples were sealed in 1 mm fused silica cuvettes. All samples were sealed while still in the humidity control box to retain a constant humidity level. Samples equilibrated under 0% relative humidity still contained approximately one water per sulfonate, ($\lambda = 1$). These samples will be referred to as "dry" Nafion. The long-term stability of the samples was monitored by FTIR spectroscopy to ensure that the cells were airtight. All experiments were performed at 25 °C. Infrared spectra were measured with an FTIR spectrometer. Fluorescence spectra were taken on a Fluorolog-3 fluorescence spectrometer. The fluorescence measurements were made at low concentration to avoid spectral distortion from emission reabsorption. The spectra were corrected for the Xe lamp intensity profile, monochromator, and photomultiplier response.

B. Time-Resolved IR Experiments. The laser system used for the time-resolved IR experiments consists of a home-built Ti:sapphire oscillator and regenerative amplifier operating at 1 kHz that pumps an OPA and a difference frequency stage to produce ~70 fs, ~4 μm IR pulses. Pulses are split into pump and probe pulses with the probe's polarization set to ~45° relative to the pump. After the sample, the components of the probe with polarization parallel and perpendicular to the pump are selected to avoid depolarization effects due to optics in the beam path.[37] Polarizers set to parallel and perpendicular are rotated into the beam using a computer-controlled filter wheel. Scans alternate between parallel and perpendicular to reduce the effects of long-term laser drift between the two polarizations. After the polarizers, a half wave plate rotates the polarization of each component to 45° prior to the entrance slit of a 0.25 m monochromator so that both parallel, $I_{||}(t)$, and perpendicular, $I_{\perp}(t)$, polarization scans experience the same diffraction efficiency from the monochromator grating. The spectrally resolved pump−probe signal is detected by a 32-element HgCdTe detector (Infrared Associates and Infrared Systems Design).

C. Time-Correlated Single-Photon Counting Experiments. A Ti:sapphire oscillator was used as the excitation source in the time-correlated single-photon counting (TCSPC) experiments. The laser wavelength was set to 790 nm, and the output beam was focused into an acousto-optic pulse selector that produced pulses at 4 MHz. The stream of pulses was frequency doubled and used for excitation. Excitation polarization was controlled by a half-wave plate placed immediately before the sample. The emitted photons were collected with a front-face geometry and passed through a fixed-angle polarizer before entering a monochromator. The photons were detected with a Hamamatsu microchannel plate detector. The instrument response function was ~45 ps fwhm. All measurements were carried out at room temperature.

The TCSPC measurements for excited-state proton-transfer dynamics were made by rotating the polarization of the excitation beam to the magic angle (54.7°) with respect to the collecting polarizer. The anisotropy measurements of MPTS were carried out by setting the excitation polarization to 0 and 90° to measure the parallel and perpendicularly polarized fluorescence decays, denoted as $I_{||}(t)$ and $I_{\perp}(t)$, respectively.

D. Anisotropy Measurements and Analysis. In both the IR pump−probe experiments and the TCSPC experiments, measurements of $I_{||}(t)$ and $I_{\perp}(t)$ can be used to isolate the contribution to the decay of the signal from excited-state population relaxation, $P(t)$, using

$$P(t) = I_{||}(t) + 2I_{\perp}(t) \tag{1}$$

and the contribution from orientational relaxation, $r(t)$ (anisotropy), using

$$r(t) = \frac{I_{||}(t) - I_{\perp}(t)}{I_{||}(t) + 2I_{\perp}(t)} = \frac{2}{5}C_2(t) \tag{2}$$

where $C_2(t)$ is the second Legendre polynomial orientational correlation function.

As we will discuss below, anisotropy measurements on water and MPTS in Nafion yield biexponential decays. There are several ways to interpret biexponential anisotropy decays. One interpretation is that the two time constants are characteristic reorientation times for two different environments. A second interpretation is based on the wobbling-in-a-cone model developed by Lipari and Szabo.[38] The wobbling-in-a-cone model was originally proposed to describe the restricted sampling of angular space by, for example, the motion of a chromophore that is tethered to a much larger molecule such as a relatively immobile macromolecule. The angular range that the group can sample is restricted by steric effects due to the macromolecule. The situation in Nafion is different, yet there are parallels that make the model useful. These parallels will be discussed in detail below for each system, but it is useful to introduce the mathematical framework that will be used in the analysis of both the IR and visible anisotropy measurements here.

In the wobbling-in-a-cone model, the motion of the molecule is restricted to a cone of semiangle θ_c, and the correlation function for the short-time motion is given by[38]

$$C_w(t) = S^2 + (1 - S^2)e^{-t/\tau_w} \tag{3}$$

Here, $C_w(t)$ is the orientational correlation function for the wobbling, S is the generalized order parameter that describes the degree of restriction, and τ_w is the time constant for the orientational motion in the cone. In the context of the wobbling-in-a-cone model, S is related to the cone half-angle, θ_c, by[38]

$$S = \frac{1}{2}(\cos\theta_c)(1 + \cos\theta_c) \tag{4}$$

In a situation where there are two independent processes contributing to orientational relaxation (a fast wobbling-in-a-cone and a longer-

(37) Tan, H.-S.; Piletic, I. R.; Fayer, M. D. *J. Opt. Soc. Am. B: Opt. Phys.* **2005**, *22*, 2009−2017.

(38) Lipari, G.; Szabo, A. *J. Am. Chem. Soc.* **1982**, *104*, 4546−4559.

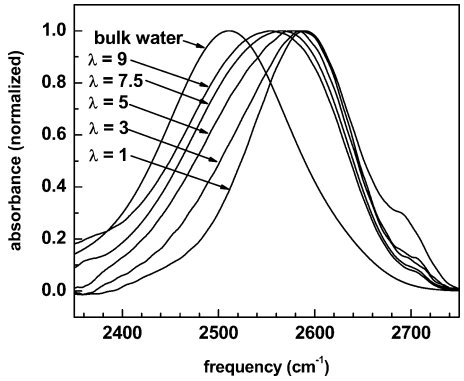

Figure 3. Normalized background-subtracted spectra of ~5% HOD in H_2O in Nafion membranes at various water contents, λ, and the spectrum of bulk water for comparison. Note that the relative amplitude of the high-frequency shoulder tends to decrease with increased water content.

time-scale complete orientational randomization), the total orientational correlation function can be expressed as

$$C_2(t) = (S^2 + (1 - S^2)e^{-t/\tau_w})e^{-t/\tau_l} \quad (5)$$

Here, τ_l is the time constant for complete orientational randomization. Within this framework, the cone half-angle, θ_c, can be extracted from the amplitude of the long-time component of the anisotropy decay, τ_l. The wobbling time constant, τ_w, is not directly measured experimentally because the short-time anisotropy contains some contribution from the long-time decay but it is related to the two measured time constants by

$$\tau_w = (\tau_s^{-1} - \tau_l^{-1})^{-1} \quad (6)$$

where τ_s is the short-time component of the anisotropy decay. The wobbling-in-a-cone model assumes that the motion in the cone is diffusive in nature with a diffusion constant, D_c, given by

$$D_c = \frac{x^2(1+x)^2\{\ln[(1+x)/2] + (1-x)/2\}}{\tau_w(1-S^2)[2(x-1)]} + \frac{(1-x)(6+8x-x^2-12x^3-7x^4)}{24\tau_w(1-S^2)} \quad (7)$$

where $x = \cos(\theta_c)$. For a system in which the long-time orientational motion obeys Gaussian diffusion, the observed decay time, τ_l, can be related to the second Legendre polynomial orientational diffusion constant by

$$D_l = \frac{1}{6\tau_l} \quad (8)$$

In the case of water, recent MD simulations have provided evidence that the long-time orientational motion is not diffusive in nature, and a more detailed description of the mechanism for long-time orientational relaxation will be given below.

III. Results and Discussion

A. Steady-State Measurements. Measurements of the steady-state infrared spectrum of water in Nafion as well as the steady-state fluorescence spectrum of HPTS in Nafion can provide important information about how the aqueous domains change with increasing hydration. Figure 3 shows the IR spectra of the O−D stretch of HOD in Nafion at a number of hydration levels with the IR spectrum of bulk water for comparison. Several trends are immediately apparent. First, at low hydration levels, the spectra are significantly blue-shifted from that of bulk water with a prominent shoulder on the high-frequency side of the line.

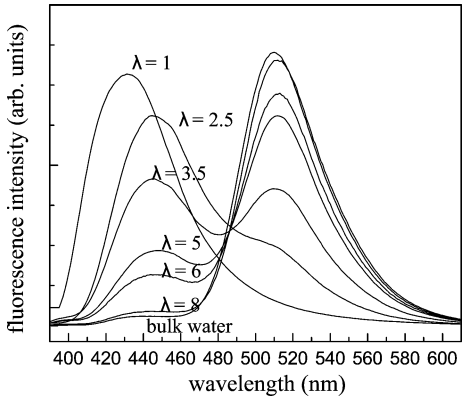

Figure 4. Steady-state fluorescence spectra of HPTS in Nafion.

At low hydration levels, most of the water is involved in solvating the sulfonate groups with a significant number of water molecules hydrogen bonding to two sulfonate groups simultaneously.[17] The high-frequency shoulder has an absorption frequency quite close to that of gas-phase HO−D, ~2724 cm^{-1}. Falk[3] and Moilanen et al.[27] interpreted this as an indication that these water molecules were experiencing a nonpolar environment and were probably in contact with the fluorocarbon backbone. MD simulations suggest that the number of water molecules in contact with the fluorocarbon is very low at all hydration levels,[17] which is inconsistent with the shoulder observed at frequencies >2700 cm^{-1}. However, simulations on a highly heterogeneous system such as Nafion are difficult, and the concentration of water in hydrophobic regions will be very sensitive to the details of the potential and the implementation of the simulation. As the hydration level of the membrane increases, the main peak of the IR spectrum shifts to the red, approaching that of bulk water but not reaching it at the highest hydration level studied. The spectra also broaden with increasing hydration, suggesting that the environment in Nafion is quite heterogeneous with many possible types and strengths of hydrogen bonds. The increasing heterogeneity in the number of hydrogen bonds per molecule has also been observed in MD simulations.[39]

The increasingly bulklike characteristics of the aqueous domains with increased hydration can also be observed in the steady-state fluorescence spectra of HPTS in Nafion (Figure 4). The fluorescence spectrum of HPTS in bulk water is also displayed in Figure 4 for comparison. The fluorescence spectra consist of two peaks at most hydration levels with the peak at 445 nm representing the population of protonated HPTS in the excited state and the peak at 510 nm representing the population of the deprotonated state. At the highest hydration level, the fluorescence spectrum is quite similar to that of bulk water with nearly all molecules transferring their proton to the solvent within the fluorescence lifetime (~5 ns). The similarity to the bulk water spectrum provides evidence that the HPTS molecule is in the aqueous domains, as far from the interfacial sulfonate groups as possible. As the hydration level decreases, there is a continuous shift toward a greater population of protonated HPTS, indicating that the water is less able to solvate the charge-separated state, and deprotonation does not happen on the time scale of the fluorescence lifetime. At the lowest hydration level, $\lambda = 1$, all of the molecules remain in their protonated states, and the fluorescence spectrum is slightly blue-shifted. The apparent blue shift is actually due to the absence of a Stokes shift in the fluorescence at $\lambda = 1$ because there is not enough water in the

(39) Blake, N. P.; Petersen, M. K.; Voth, G. A.; Metiu, H. *J. Phys. Chem. B* **2005**, *109*, 24244−24253.

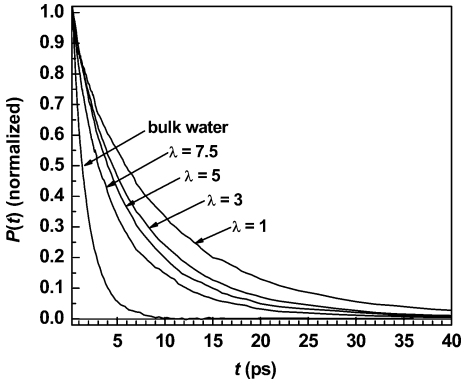

Figure 5. Vibrational lifetime decays at various water contents, λ.

Table 1. Vibrational Lifetimes of Water in Nafion at Various Hydration Levels

λ	τ_1 (ps)	τ_2 (ps)
1	5.1	11
3	3.2	8.6
5	2.3	6.5
7.5	2.0	5.9

membrane to solvate and stabilize the excited state. The difficulty in transferring a proton to the solvent at intermediate hydration can be understood in terms of the infrared spectra. At low hydration levels, the IR spectra indicate that most of the water molecules are involved in solvating the sulfonate groups and possibly bridging two sulfonate groups. These water molecules that are strongly interacting with the interface have very low mobility, and because water mobility is crucial to stabilizing the charge-separated state of the photoacid, the extent of excited-state deprotonation is reduced.

B. Changing Structure of the Aqueous Domains. The steady-state spectra show that the aqueous domains swell and the water inside becomes more bulklike as the hydration level increases. However, more detailed information regarding the changing nature of the interfacial regions and the irregular swelling of the aqueous domains is provided by measurements of the vibrational population relaxation of water and the time-resolved anisotropy decay of MPTS.

Vibrational relaxation is sensitive to the local fluctuating forces that act on a water molecule as well as the availability of vibrational modes at lower energy that can receive the hydroxyl stretch energy and eventually dissipate the energy into the bath as heat.[40] Changes in either of these factors can affect the vibrational lifetime, and although it is difficult to pinpoint the exact cause of a change in the vibrational lifetime, its sensitivity to local factors makes it a useful probe of changes in the local environment of a water molecule. Figure 5 shows how the vibrational lifetime changes with the hydration level of the membrane. The data presented here have been corrected for a small, well-documented thermal offset using standard procedures.[41,42] Vibrational relaxation is biexponential at all hydration levels, indicating the presence of at least two distinct environments. However, the characteristic relaxation times of the two environments change as the hydration level changes, indicating that the swelling of the hydrophilic domains is not uniform. Time constants for vibrational relaxation are given in Table 1.

In previous experiments on water in AOT reverse micelles, the vibrational relaxation was found to obey a core/shell model

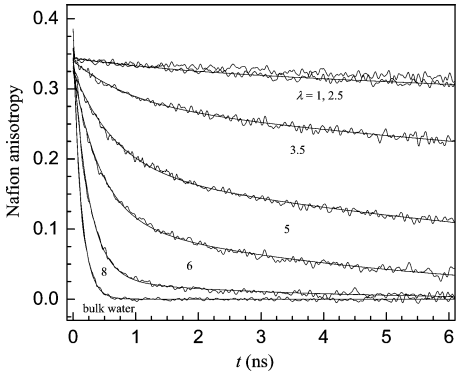

Figure 6. Anisotropy decays of MPTS in Nafion. Solid lines are biexponential fits to the data.

in which the fast relaxation time corresponded to bulklike water in the micelle core and the slow relaxation time corresponded to interfacial water interacting with the sulfonate groups.[30] In the AOT reverse micelles, the time constants of these two components did not depend on the size of the reverse micelle, indicating that the change in size preserved the nature of the core water and the interfacial water.

In Nafion, the picture is more complex. The IR spectra and MD simulations clearly show that the interfacial region of the aqueous domains reorganizes as the hydration level changes. This rearrangement could affect the vibrational lifetime of water by changing the nature of the interactions between water and the interface (e.g., by reducing the number of water molecules bridging two sulfonate groups). In addition, the size and shape of the hydrophilic domains are unlikely to be as uniform as AOT reverse micelles. The irregularity in the size of the water channels could also contribute to the presence of multiple decay times for the vibrational relaxation. It is likely that both of these factors play a role in determining the observed vibrational lifetime. Interestingly, only two relaxation times are required to provide good fits to the vibrational lifetime at all absorption frequencies for a given hydration level.[28] As the observation wavelength shifts from red to blue, the fraction of the decay due to the slow component increases from ~0 to ~1 on the far blue side of the line. In AOT reverse micelles, the slow component of the observed biexponential population decay is assigned to water molecules associated with the sulfonate head groups. The AOT observations indicate that in Nafion the biexponential decay is composed of hydroxyls associated with head groups (blue side of the line) and those not associated with head groups (red side of the line). As the Nafion hydration level is changed, both the associated and unassociated local environments change, producing distinct biexponential decays at each hydration level.

The time-dependent anisotropy of MPTS is sensitive to the orientational mobility of the probe molecule. Because MPTS cannot undergo excited-state proton transfer, its fluorescence decays only through population relaxation and orientational relaxation. The fluorescence lifetime (population relaxation) of MPTS in Nafion is single-exponential and frequency-independent. The anisotropy (eq 2) provides a method for tracking the orientational motions of MPTS free of population relaxation. Anisotropy decays of MPTS in Nafion at various levels of hydration are shown in Figure 6. The time scale of orientational relaxation changes dramatically with the hydration level. Clearly, the orientational mobility of MPTS is highly restricted at low hydration levels with exceedingly slow reorientation occurring at $\lambda = 1$ and 2.5. This indicates that the aqueous domains are similar in size to the MPTS molecule, ~0.5 nm. As the hydration

(40) Kenkre, V. M.; Tokmakoff, A.; Fayer, M. D. *J. Chem. Phys.* **1994**, *101*, 10618.
(41) Steinel, T.; Asbury, J. B.; Fayer, M. D. *J. Phys. Chem. A* **2004**, *108*, 10957−10964.
(42) Rezus, Y. L. A.; Bakker, H. J. *J. Chem. Phys.* **2005**, *123*, 114502.

Table 2. Orientational Relaxation Parameters for MPTS in Nafion[a]

λ	A_s	τ_s (ns)	A_l	τ_l (ns)	θ_c (deg)	D_c (ns^{-1})	D_l (ns^{-1})
2.5	0.02	1.8	0.33	100	21	0.0057	0.0018
3.5	0.06	0.92	0.28	30	28	0.039	0.0057
5	0.14	0.68	0.18	11.7	40	0.13	0.014
6	0.21	0.45	0.11	5.1	50	0.30	0.033
8	0.32	0.25	0.03	3.1	67	0.85	0.055
bulk	0.36	0.13					7.7

[a] A_s is the short-component amplitude, τ_s is the short-time constant, A_l is the long-component amplitude, τ_l is the long-time constant, θ_c is the cone angle, D_c is the diffusion constant in the cone, and D_l is the long-time constant for Gaussian diffusion.

level increases, the ability of the MPTS molecule to rotate increases, although even at $\lambda = 8$ there is a small long-lived anisotropy.

The anisotropy decays of MPTS cannot be fit well by a single exponential at any hydration level. There are two ways to interpret the biexponential anisotropy decays for MPTS in Nafion: the heterogeneity of the channel size or wobbling-in-a-cone followed by compete orientational relaxation. It is possible that both factors play a role in determining the orientational dynamics. The first interpretation is that the biexponential anisotropy decay is representative of MPTS molecules residing in domains of two different average sizes. When MPTS is in a relatively large water channel, it is able to reorient relatively quickly, but when it is in a smaller channel, the reorientation is slowed. Because the steady-state fluorescence spectrum (Figure 2) shows that HPTS (and MPTS) resides in the aqueous domains, there is no reason to suspect that the slower component of the anisotropy is due to MPTS molecules buried in the interface. Although the anisotropy decay can be fit as a biexponential, this fact does not necessarily indicate two unique environments because two fairly broad distributions of relaxation times ($\pm\sim$50%) centered about an average fast relaxation time and an average slow relaxation time will also produce data that can be fit very well as a biexponential decay. It does suggest that at all hydration levels at which MPTS is able to rotate significantly ($\lambda \geq 2.5$) there are both larger and smaller aqueous regions in Nafion.

Another interpretation of the biexponential anisotropy decay of MPTS in Nafion is based on the wobbling-in-a-cone model described above. In this model, the picture is that the complicated and tortuous channels that make up the hydrophilic domains restrict the orientational motion of the MPTS molecule on a short time scale. MD simulations show that the interfacial regions of the aqueous domains in Nafion are quite irregular,[39] and it is reasonable to imagine that the orientational motion of an MPTS molecule could become frustrated by the twists, turns, and protrusions of the channels in Nafion. On a much longer time scale, the MPTS molecule is able to sample more of its orientational space through random fluctuations that allow it to move past some of the obstacles that originally restricted its orientational motion.

Orientational relaxation decay parameters for MPTS in Nafion are given in Table 2. As the hydration level of the membrane increases, several changes occur. The time constants for both the fast component and slow component become faster, and the amplitude of the fast component becomes larger relative to that of the slow component. These changes in the time constant are representative of physical changes occurring in the membrane.

Either the heterogeneous two-domain-size picture or the wobbling-in-the-cone model is consistent with the observed changes in time constants and the physical picture of increasing overall domain size with increased hydration. In the two-domain-size picture, both domain sizes become larger, as shown by the decreasing time constants for both components, and the relative amount of the larger regions increases, as shown by the increasing fraction of the amplitude in the fast component. In the context of the wobbling-in-a-cone model, the larger aqueous domains allow MPTS molecules to sample a larger range of angles on a shorter time scale before their motion is restricted by interactions with the complex topology of the channel walls. This is reflected in the increasing cone angles and cone diffusion constants (eq 7) given in Table 2. Larger channels also increase the probability that fluctuations of the MPTS orientation and possible fluctuations of the interfacial topology will enable MPTS to escape from orientational traps more readily, resulting in an increased long-time diffusion constant (eq 8). More experimental work may be able to determine which of the two models gives rise to the biexponential anisotropy decays observed for MPTS.

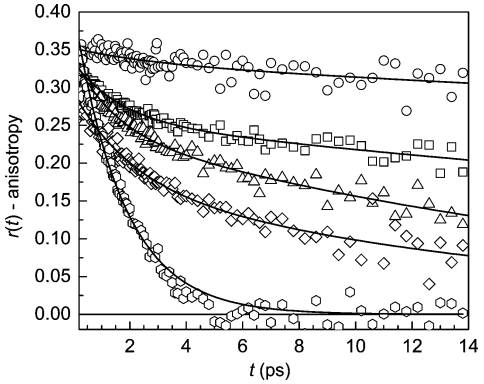

Figure 7. Anisotropy decays at the peak of the absorption spectrum for $\lambda = 1$ (○), 3 (□), 5 (△), and 7.5 (◇). The anisotropy decay of bulk water (⬡) is shown for comparison. Solid lines are fits to the data. All Nafion samples were fit using biexponential decays. Water was fit using a single-exponential decay.

C. Water Dynamics and Proton Transfer. The varying sizes of the hydrophilic domains and their complicated topology have a substantial affect on the nature and dynamics of the hydrogen-bonding network of water. Local observables such as the IR spectra and vibrational lifetime show how the nature of the hydrogen bonds change as the membrane hydration changes. The time-resolved anisotropy decay of water in Nafion provides a tool for observing the dynamics of the hydrogen-bonding network. The anisotropy measures the reorientational dynamics of the water molecules. Complete orientational randomization requires the concerted rearrangement of the hydrogen bond network, a process that requires the formation and breakage of hydrogen bonds. Factors that influence the ability of water molecules to break and form hydrogen bonds, which change with hydration, will manifest themselves in λ-dependent anisotropy decays.

Figure 7 shows the anisotropy decays of water in Nafion at various levels of hydration and the anisotropy decay of bulk water for comparison. The anisotropy decays are substantially slower in Nafion than in water at all hydration levels, and at the lowest hydration level, $\lambda = 1$, virtually no reorientation occurs on the time scale of the measurement, which is limited by the vibrational lifetime. The solid lines in Figure 7 are biexponential fits to the data. All of the anisotropy decays display some common features. There is an ultrafast inertial decay of the anisotropy that occurs during the first $\sim$100 fs and is obscured by a strong nonresonant signal around $t = 0$. After the inertial decay, the anisotropy decays with a fast component of $\sim$1.5 ps and a much slower component with a time constant that varies strongly with the membrane hydration level.

Table 3. Orientational Relaxation Parameters for Water in Nafion[a]

λ	A_s	τ_w (ps)	θ_c (deg)	A_l	τ (ps)
1	0.02 ± 0.02	3 ± 3	25	0.33 ± 0.02	∞
3	0.08 ± 0.01	1.8 ± 0.2	33	0.25 ± 0.01	63 ± 10
5	0.10 ± 0.01	1.3 ± 0.2	33	0.24 ± 0.01	22 ± 2
7.5	0.12 ± 0.02	1.9 ± 0.4	40	0.17 ± 0.02	17 ± 3
bulk	0.34 ± 0.01	2.6 ± 0.1			

[a] A_s is the short-component amplitude, τ_w is the wobbling time constant, θ_c is the cone angle, A_l is the long-component amplitude, and τ is the jump diffusion time constant.

The biexponential decay (following the ultrafast inertial component) can be described by a wobbling-in-a-cone model,[28,38] followed by complete orientational relaxation. As discussed above, the wobbling-in-a-cone model was originally developed to describe the restricted sampling of angular space by a large molecule. Although the situation in water is different, there are parallels that make the model physically applicable. On a time scale that is short compared to that for concerted hydrogen bond rearrangement for complete orientational relaxation, the angular motions of a water molecule are restricted by the intact hydrogen bond network. The OD bond vector (approximately the direction of the transition dipole) can still undergo orientational relaxation but only in a limited range of angles, the cone. The mathematical framework of the wobbling-in-a-cone model was given above.

As early as the 1970s, MD simulations suggested that the mechanism for the complete reorientation of water molecules was not diffusive in nature but instead involved large-amplitude angular jumps.[43] It was further suggested that the transition state for reorientation should involve bifurcated hydrogen bonds.[44] Recently, Laage and Hynes put these two ideas together in describing a mechanism for bulk water in which the transition state for large-amplitude reorientational jumps involves a bifurcated hydrogen bond between the reorienting water molecule and the initial and final acceptor molecules.[45] The time constant for jump diffusion measured in the IR pump−probe anisotropy experiment (eqs 2 and 5) is

$$\tau_l = \frac{\tau_j}{\left(1 - 0.2\frac{\sin 2.5\theta_0}{\sin \theta_0/2}\right)} \qquad (9)$$

where τ_j is the time between jumps and θ_0 is the jump angle. During the time between these large-amplitude jumps, the angular motion of the water molecule is restricted by the hydrogen bonds it forms with its neighbors. This hydrogen-bonding cage restricts the angular motion of the water molecules on a short time scale much like a macromolecule restricts the motion of a group tethered to it. Unlike the macromolecule situation, water is able to reorient on a longer time scale as a result of dynamical changes in the hydrogen-bonding network that lead to the breakup of the original hydrogen-bonding configuration.

Because the large-amplitude jump reorientations depend on changes in the coordination of water molecules in the first and second solvation shells of the HOD molecule, it is safe to assume that the wobbling motion of the OD bond is statistically independent from the jumps,[45] and the overall correlation function can be written in the form of eq 5. In the case of water, τ_l in eq 5 is the jump reorientation time constant given by eq 9.

Table 3 lists the measured amplitudes, A_s and A_l, and time constants, τ_w and τ_l, for the anisotropy decay at the four hydration levels as well as the cone angles, θ_c. Separating the jump rate, $1/\tau_j$, from the jump angle, θ_0, is not possible from the measurement of τ_l because there are two unknowns in the equation (eq 9). However, to obtain an idea of the time scale of τ_j, the value obtained for θ_0 from the MD simulations of bulk water of $\sim 60°$ [45] can be used. Then, from eq 9, $\tau_j = 0.8\tau_l$. Thus, the values reported for τ_l in Table 3 are closely related to the jump times, which can be interpreted as the time scale for hydrogen bond network rearrangement.

In section III.B, the biexponential anisotropy decay for MPTS was interpreted in two ways: the presence of larger and smaller hydrophilic domain sizes and the wobbling-in-a-cone model. However, there are strong physical reasons based on simulations of bulk water[45] and experiments and simulations of water in reverse micelles[30,31,46] that support the wobbling-in-a-cone model for water reorientational dynamics in Nafion even if there is size heterogeneity. The fast decay times reported in Table 3 for water are all fairly similar within experimental error and are all faster than the decay time for bulk water. A fast decay time, faster than bulk water, has been observed in other systems involving confined water,[30,47,48] and the decay times are consistently in the range of $\sim 1-2$ ps regardless of the size of the confining region. This consistent result supports the conclusion that the fast anisotropy decay is due to motion within an initial hydrogen-bonding configuration and does not depend significantly on the size of the hydrophilic domain. The long-time anisotropy decay is sensitive to the size of the confining region. However, the OD vibrational lifetime limits the experimental window to $\sim 10-15$ ps. Therefore, we may not be able to distinguish that there are possibly two contributions to the long-time decay. It is possible that the observed long-time anisotropy decay for water in Nafion is an average over larger and smaller domains that may be present at a given hydration level.

There are several trends in the anisotropy parameters reported in Table 3. First, the amplitude of the short-time component, A_s, increases with increased hydration, leading to larger cone angles for higher hydration levels. This means that the water molecules are able to sample more of their orientational space on a fast time scale. At the lowest hydration level ($\lambda = 1$), virtually no reorientation occurs after the small-amplitude short-time component. Whereas the time constant for the fast component is similar for all four samples, the long-time component, τ_l, becomes significantly faster for the higher hydration levels. If the reorientational angular displacements that water molecules make during a jump are similar at each of the hydrations, then the increase in the decay of the long component indicates that the average jump rate is increasing with increased hydration. In the case of $\lambda = 1$, so little water is present in the membrane that it is never possible to find a new hydrogen bond acceptor, so no jumps occur on the time scale of the experiment.

Complete reorientation of water molecules requires the breaking and forming of hydrogen bonds, which depends on the concerted motion of several water molecules to lower the energy barrier of the hydrogen bond transition state. Although the local reorientational event requires the participation of water molecules in the first and second solvation shells of the reorienting molecule, the ability of these molecules to accept a hydrogen bond depends on the dynamics of their own solvation shells. The necessity of

(43) O'Reilly, D. E. *J. Chem. Phys.* **1974**, *60*, 1607−1618.
(44) De Santis, A.; Rocca, D. *J. Chem. Phys.* **1997**, *107*, 10096−10101.
(45) Laage, D.; Hynes, J. T. *Science* **2006**, *311*, 832−835.
(46) Faeder, J.; Ladanyi, B. M. *J. Phys. Chem. B* **2000**, *104*, 1033−1046.
(47) Piletic, I. R.; Moilanen, D. E.; Levinger, N. E.; Fayer, M. D. *J. Am. Chem. Soc.* **2006**, *128*, 10366−10367.
(48) Moilanen, D. E.; Levinger, N. E.; Spry, D. B.; Fayer, M. D. *J. Am. Chem. Soc.* **2007**, *129*, 14311−14318.

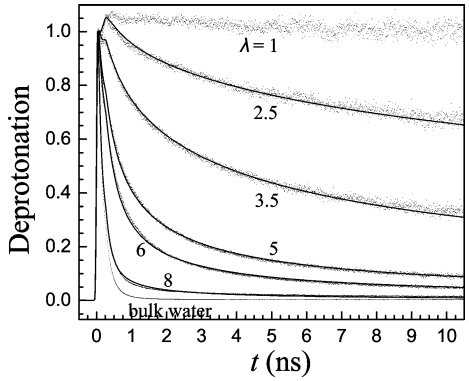

Figure 8. Fluorescence decays of HPTS in the water channels of Nafion at various water contents, λ. Solid lines are fits to the data based on the kinetic model described in the text.

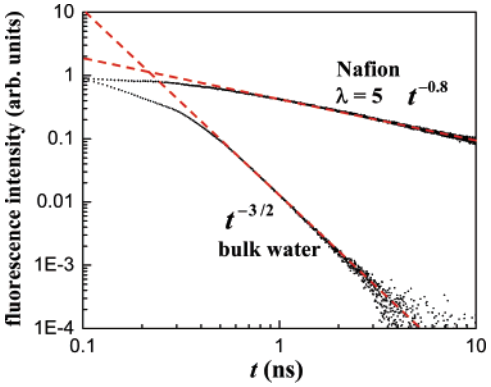

Figure 9. Protonated excited-state population of HPTS corrected for lifetime in bulk water and $\lambda = 5$ Nafion. The dashed lines are included to show the $t^{-3/2}$ power law decay in water and the $\sim t^{-0.8}$ power law decay in Nafion.

cooperative motion means that the long-time anisotropy decay is sensitive to the hydrogen bond dynamics of a group of water molecules, not the local environment of a single water molecule. The short-time-scale wobbling-in-a-cone motion is also determined by the nature of the local hydrogen-bonding configuration of the wobbling OD hydroxyl group under observation.

The effect of the slowing water dynamics on proton transfer can be observed by studying the excited-state proton transfer (ESPT) of HPTS in Nafion. Figure 8 shows the fluorescence decay of the HPTS protonated state due to proton transfer, with the excited-state lifetime contribution of HPTS in water (5.4 ns) removed.[49] At low hydrations, the excited-state lifetime was adjusted so that the proton-transfer kinetics were consistent with the steady-state fluorescence measurements. The steady-state fluorescence measurements give the time-integrated proton-transfer kinetics. Therefore, integrating the time-resolved proton-transfer kinetics (from TCSPC) and comparing the results to the time-integrated fluorescence measurements (the same ratio of protonated/deprotonated fluorescence) provides the necessary information to make corrections to the fluorescence lifetime.

The decay of the curves in Figure 8 demonstrates that the proton has successfully moved away from the HPTS molecule. The trends in the ESPT follow the trends in the anisotropy decays of water quite closely. At low hydration, no proton transfer occurs because there is very little water in the membrane and what is present is unable to reorient to solvate the proton. As the hydration level increases and the orientational mobility of the water molecules increases, the extent of proton transfer also increases although it never reaches that of HPTS in bulk water.

The dissociation dynamics of HPTS have been studied extensively by a number of authors.[49−53] Proton dissociation leaves HPTS in an electronic excited state. Because of HPTS's −4 charge in the deprotonated state, the Columbic attraction for the dissociated proton is large, and the recombination is substantial and fast in the excited state. (The ground-state recombination of the HPTS anion with a free hydronium ion is among the fastest measured bimolecular reactions.[54])

The most common approach to modeling geminate recombination reactions is to employ the diffusion (Smoluchowski) equation with back-reaction boundary conditions.[51,55,56] This technique has been used to model the dynamics of photoacids in a number of different environments, including AOT reverse micelles.[16,57] This method requires knowledge of the system's geometry, dielectric constant, proton diffusion constant, ion screening effects, and interactions at the boundary, all of which are unknown for Nafion. Nonetheless, it is possible to obtain substantial information about proton transport by comparing the proton transport dynamics of HPTS in AOT, Nafion, and bulk water through the use of an empirical model.

The long-time recombination rate, $k_{-1}(t)$, of two particles with a Coulomb potential in an infinite system has been obtained by solving the Smoluchowski equation analytically[58] and has the form

$$k_{-1}(t) = k_{-1}t^{-d/2} \tag{10}$$

where d is the dimensionality of the infinite system. For the 3D case, there is a $t^{-3/2}$ power law with

$$k_{-1} = \frac{R_D e^{-R_D/r_o}}{\sqrt{D}} \tag{11}$$

In eq 11, D is the combined diffusion constants of the two ions, R_D is the Debye radius, and r_o is the initial separation of the two ions immediately after dissociation has occurred.[52,58]

At long times relative to the initial dissociation time ($\sim 1/k_1$ where k_1 is the forward transfer rate constant, see eq 12 below), the recombination kinetics determine the probability of finding the system in the protonated state of HPTS. In systems where free diffusion is possible in three dimensions, the time dependence goes as $t^{-3/2}$, the so-called $^3/_2$ power law. This was observed previously[59] and recently confirmed for bulk water in a comparative study of HPTS in bulk water, AOT reverse micelles, and Nafion.[16] The $t^{-3/2}$ power law for bulk water is shown in Figure 9. In that study, it was observed that the long-time proton-transfer kinetics of HPTS in AOT reverse micelles and in Nafion displayed a power law dependence, $t^{-0.8}$. The data for Nafion, $\lambda = 5$, is also shown in Figure 9. The influences of finite volume on excitation transport systems that involve a return to the initially excited molecule demonstrate the substantial effect that finite volume has on transport observables.[60−63] The −0.8 exponent

(49) Leiderman, P.; Genosar, L.; Huppert, D. *J. Phys. Chem. A* **2005**, *109*, 5965−5977.
(50) Mohammed, O. F.; Pines, D.; Dreyer, J.; Pines, E.; Nibbering, E. T. J. *Science* **2005**, *310*, 83−86.
(51) Agmon, N. *J. Phys. Chem. A* **2005**, *109*, 13−35.
(52) Pines, E.; Huppert, D. *Chem. Phys. Lett.* **1986**, *126*, 88−91.
(53) Spry, D. B.; Goun, A.; Fayer, M. D. *J. Phys. Chem. A* **2007**, *111*, 230−237.
(54) Förster, T.; Volker, S. *Chem. Phys. Lett.* **1975**, *34*, 1−6.
(55) Agmon, N.; Szabo, A. *J. Chem. Phys.* **1990**, *92*, 5270−5284.
(56) Goun, A.; Glusac, K.; Fayer, M. D. *J. Chem. Phys.* **2006**, *124*, 084504.
(57) Cohen, B.; Huppert, D.; Solntsev, K. M.; Tsfadia, Y.; Nachliel, E.; Gutman, M. *J. Am. Chem. Soc.* **2001**, *124*, 7539−7547.
(58) Hong, K. M.; Noolandi, J. *J. Chem. Phys.* **1978**, *68*, 5163−5171.
(59) Pines, E.; Huppert, D. *J. Chem. Phys.* **1986**, *84*, 3576−3577.

Table 4. ESPT Rate Constants of HPTS in Nafion

λ	k_1	k_{-1}
8	9.1	0.36
6	3.8	0.93
5	3.5	1.7
3.5	1.8	5.1
2.5	0.43	8.1

is observed for both Nafion and AOT reverse micelles over a range of water content. Therefore, it does not appear that the exponent is caused by the specific topology of the system. It may be due to the interaction of the protons with the interface, which could produce a distribution of recombination times not controlled strictly by diffusion in water.

$$\begin{pmatrix} \frac{d[RO^*H]}{dt} \\ \frac{d[RO^{*-}]}{dt} \end{pmatrix} = \begin{pmatrix} -k_1 & k_{-1}t^{-0.8}[RO^{*-}] \\ k_1 & -k_{-1}t^{-0.8}[RO^{*-}] \end{pmatrix} \begin{pmatrix} [RO^*H] \\ [RO^{*-}] \end{pmatrix} \quad (12)$$

To describe the data for both AOT and Nafion, the reverse reaction rate was modeled as $k_{-1}(t) = k_{-1}t^{-0.8}$. The population dynamics of the lifetime-corrected protonated state, RO^*H, in Nafion can then be fit to the rate equations.

This kinetic scheme produces an exponential decay at short times and a power law decay at long times. Equation 12 was integrated and fit to the TCSPC data in Figure 8 by least-squares regression. The resulting fits convolved with the instrument response are the solid lines in Figure 8. The values of the rate constants for the proton-transfer kinetics of HPTS in Nafion are given in Table 4. The time scale for the initial exponential decay of the protonated state at the highest hydration level ($1/k_1$) is ~100 ps, which is very close to the value of ~90 ps reported for bulk water.[49,53,59]

The trends in the proton-transfer kinetics can be understood in terms of the water dynamics. As the hydration level is reduced, the rate of forward proton transfer decreases, and the rate of the back reaction increases. The forward rate decreases as the size of the water pool becomes smaller because water cannot solvate the charge pair formed in the proton-transfer reaction as effectively. This reduction in the forward rate is likely due to the reduction in the rate of hydrogen bond rearrangement of the water as well as the simultaneous need for the water molecules to solvate the ionic sulfonate groups that are part of the interfacial region. Solvation of the proton requires hydrogen bond network structural reorganization. The results for the anisotropy decays of water in Nafion presented above as well as experiments on water in AOT show that the time scale of hydrogen bond structural rearrangement increases substantially as the sizes of the water regions become small.[27,28,30,31,64,65] This suggests that the ability of the nanoscopic water to rapidly reconfigure to accommodate a newly generated proton is reduced. The back reaction, or k_{-1}, increases as the hydration level decreases primarily because the proton diffusion constant is highly sensitive to the hydrogen-bonding environment. Again, as the water regions shrink in size and water molecules become less mobile, they are less able to structurally rearrange their hydrogen-bonding network to permit proton transport. The decrease in the proton diffusion constant can be related to the increase in the back-reaction rate constant by eq 11. Measurements of the proton conductivity relative to the hydration level of Nafion show that the proton diffusion constant is greatly reduced at low water content, which supports the interpretation given here.[4]

IV. Concluding Remarks

The complicated environment in the hydrophilic domains of Nafion fuel cell membranes was studied by a combination of infrared and visible spectroscopy. Infrared spectroscopy of dilute HOD in H_2O in Nafion provides a tool to probe the nature of the hydrogen-bonding network in Nafion and the interactions of water molecules with the sulfonate groups at the interface. Visible spectroscopy of the photoacid, HPTS, permits a direct measurement of the proton-transfer kinetics in the hydrophilic domains of Nafion. Steady-state spectroscopy of water and HPTS shows that the aqueous domains in Nafion grow larger and more bulklike as the hydration level increases. A restructuring of the membrane interface associated with a decrease in the number of water molecules bridging two sulfonate groups may occur above $\lambda = 5$. The vibrational lifetime of water in Nafion provides evidence that the hydroxyl of water exists in two environments and that the characteristics of the environments change as the membrane hydration changes. This result is in agreement with the observation from the steady-state spectra that indicate a rearrangement of the interfacial region. Measurements of the orientational motions of MPTS show that at any hydration level the aqueous domains do not have a single size, further highlighting the heterogeneity of the hydrophilic domains.

The dynamics of water in Nafion slow significantly as the hydration level of the membrane decreases, indicating that the hydrogen-bonding network is strongly perturbed by the confining effects of the interface. Both steady-state and time-resolved measurements of proton transfer show that the extent of nanoscopic excited-state proton transfer is greatly reduced at low membrane hydration levels. The proton-transfer kinetics depend strongly on the ability of water molecules to rearrange in order to stabilize the charge-separated excited state of HPTS. A comparison of the dynamics of water to the kinetics of proton transfer shows a strong correlation between slowing water dynamics and decreasing proton transfer.

In fuel cells, the purpose of a Nafion membrane is to transport protons from the anode to the cathode to complete the electrochemical circuit. Understanding the factors that influence proton transport on nanoscopic distance scales should be useful in developing new and more effective membranes. Clearly, the hydration level of the membrane plays the most important role, but at any given hydration level, the topology of the system, the nature of the interface, and the distribution of sizes of the hydrophilic domains are also important factors. The measurements described above show how all of these factors affect proton-transfer processes and provide a molecular-level picture of the aqueous domains in Nafion.

Acknowledgment. This work was supported by the Department of Energy (DE-FG03-84ER13251) and the National Science Foundation (DMR 0652232). D.E.M. thanks the NDSEG for a graduate fellowship.

LA703358A

(60) Ediger, M. D.; Fayer, M. D. *J. Chem. Phys.* **1983**, *78*, 2518−2524.
(61) Ediger, M. D.; Fayer, M. D. *J. Phys. Chem.* **1984**, *88*, 6108−6116.
(62) Baumann, J.; Fayer, M. D. *J. Chem. Phys.* **1986**, *85*, 4087−4107.
(63) Petersen, K. A.; Fayer, M. D. *J. Chem. Phys.* **1986**, *85*, 4702−4711.
(64) Tan, H.-S.; Piletic, I. R.; Riter, R. E.; Levinger, N. E.; Fayer, M. D. *Phys. Rev. Lett.* **2004**, *94*, 057405(4).
(65) Piletic, I. R.; Tan, H.-S.; Fayer, M. D. *J. Phys. Chem. B* **2005**, *109*, 21273−21284.